Tuning thermal conduction via extended defects in graphene

Huaqing Huang,[1] Yong Xu,[1,2,*] Xiaolong Zou,[1] Jian Wu,[1] and Wenhui Duan[1,2,†]

[1]*Department of Physics and State Key Laboratory of Low-Dimensional Quantum Physics, Tsinghua University,
Beijing 100084, People's Republic of China*

[2]*Institute for Advanced Study, Tsinghua University, Beijing 100084, People's Republic of China*

Designing materials for desired thermal conduction can be achieved via extended defects. We theoretically demonstrate the concept by investigating thermal transport in graphene nanoribbons (GNRs) with the extended line defects observed by recent experiments. Our nonequilibrium Green's function study excluding phonon-phonon interactions finds that thermal conductance can be tuned over wide ranges (more than 50% at room temperature), by controlling the orientation and the bond configuration of the embedded extended defect. Further transmission analysis reveals that the thermal-conduction tuning is attributed to two fundamentally different mechanisms, via modifying the phonon dispersion and/or tailoring the strength of defect scattering. The finding, applicable to other materials, provides useful guidance for designing materials with desired thermal conduction.

PACS number(s): 44.10.+i, 65.80.Ck, 63.20.kp

I. INTRODUCTION

Optimizing thermal transport properties of materials is of crucial importance to many applications. For instance, materials of high thermal conductivity are requisite for solving the serious heat dissipation in ever-smaller integrated circuits,[1] while materials of low thermal conductivity are required for improving the thermal insulation in high-power engines[2] as well as for achieving high thermoelectric efficiency that demands simultaneously a large power factor.[3] All these require efficient approaches to tune thermal conduction.

For this purpose, various methods have been proposed. According to the mechanism of thermal conduction tuning, they can, in principle, be classified into two groups. One group tailors thermal conduction by adjusting the phonon structure (i.e., the phonon dispersion), for instance, by utilizing superlattice or nanostructuring.[4,5] The other group tunes thermal conduction by controlling the strength of phonon scattering. For example, introducing point scatterers (such as isotope impurities and atomic substitutions) can block the transport of short-wavelength phonons,[6–12] embedding nanoparticles in bulk materials can scatter phonons in the mid- to long-wavelength range,[13] whereas the rough boundary of nanowires can induce strong phonon scattering in the long-wavelength range.[14] Here we propose to tune thermal conductance via extended defects. As we will show, both mechanisms (i.e., tailoring the phonon structure and adjusting the strength of phonon scattering) take effects in this approach, and thermal conductance can be tuned over wide ranges by embedding extended defects.

To demonstrate the concept, we select graphene nanoribbons (GNRs) with extended defects as example systems for our theoretical study. Due to its unique electronic[15] and thermal[16,17] properties, graphene shows promising applications in nanoelectronics and thermal management. GNRs, which are building blocks of graphene-based devices,[18] have attracted extensive research interest. High-quality GNRs with well-controlled ribbon width and edge shape can be experimentally produced by cutting graphene sheets[19] or by unzipping carbon nanotubes.[20] On the other hand, various extended defects are inevitably to be introduced into graphene during the growth process, possibly due to the substrate imperfections and kinetic factors.[21,22] Meanwhile, benefitting from recent experimental progress,[23] a precise control over the structure of extended defects becomes feasible in graphene, while the existence of extended defects like grain boundaries has been theoretically found to significantly affect the thermal transport behavior in graphene or in GNRs.[24–26] More importantly, for extended defects, there is an extra freedom of relative orientation between the defect and the transport direction, which enables an efficient tuning over thermal conductance, as we will demonstrate.

In this study, we systematically investigated the influence of extended line defects on thermal transport in GNRs, using the nonequilibrium Green's function (NEGF) method[27–30] without phonon-phonon interactions. Our calculations show that thermal conductance of GNRs can be tuned over wide ranges, over 50% at room temperature, by controlling the direction and bond configuration of the embedded extended defect. The result clearly demonstrates that embedding extended defects can be used to effectively control thermal conduction.

II. MODEL AND METHOD

We performed atomic scale simulations on quantum thermal transport by the NEGF method,[27–30] with quantum effects fully included. The interatomic interactions were described by the second-generation reactive empirical bond order potential[31] as implemented in the "General Utility Lattice Program",[32] which gives phonon modes of GNRs in good agreement with density-functional theory calculations.[33] Thermal conductance contributed by electrons is not considered since all sub-10-nm GNRs are experimentally found to be semiconducting.[19] Phonon-phonon and electron-phonon interactions were neglected here, because they are not relevant to the present discussion on the influence of structural defects on thermal transport, and they are important only when the transport length is comparable to or larger than the phonon mean free path, which is ∼775 nm at room temperature in graphene.[34] The transport system [like the ones in Figs. 1(a) and 1(b)] consists of a center part and two semi-infinite thermal leads composed of GNRs on the left and right. The thermal
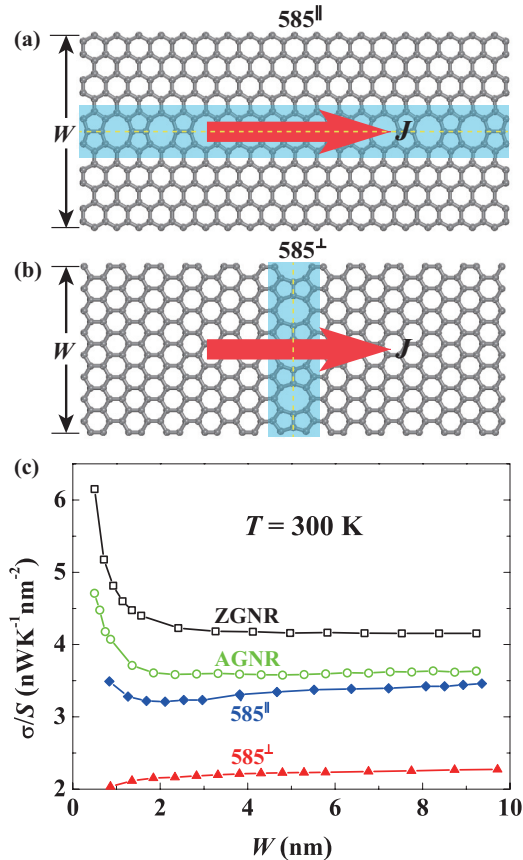
FIG. 1. (Color online) (a), (b) Schematic of thermal transport in graphene nanoribbons (GNRs) of width W with an extended "585" defect that consists of a pair of pentagons and one octagon periodically repeated along the dislocation line (denoted by the yellow dashed line). The direction of thermal current J (denoted by the red arrow) is (a) parallel and (b) perpendicular to the dislocation line, labeled by "585$^{\parallel}$" and "585$^{\perp}$", respectively. (c) Thermal conductance per unit area (σ/S) at 300 K versus W for pristine zigzag GNR (ZGNR), "585$^{\parallel}$", pristine armchair GNR (AGNR), and "585$^{\perp}$".

leads have periodic structures and thus no phonon scattering within them. The center part that is the region of interest should be large enough (i) to decouple the two thermal leads and (ii) to include all the structural defects that cause phonon scattering. In the center part, we put the defects that scatter phonons in the middle and included buffer layers on each side which have a similar structure to the neighboring thermal leads. The length of the buffer layer was selected to be ~1 nm, and further increasing its length was tested to have negligible influence on the calculated results.

The infinite but aperiodic systems were modeled by two separate steps. The first step is to relax periodic systems composed of the same structure as the thermal leads and then to calculate force constant matrices between thermal leads themselves. The second step is to consider a finite transport system including the center part with the defect and finite but long enough (e.g., 5 nm here) parts of thermal leads whose configurations were relaxed in the previous step. In this step only the structure of the center part is relaxed and then force constant matrices between the center part and the two thermal leads are computed. In the NEGF method we used the reduced

force constant matrix D as the phonon Hamiltonian.[35] The matrix element $D_{ij} = \Phi_{ij}/\sqrt{M_i M_j}$, where M_i is the mass of atom i, and Φ_{ij} is the force constant between atom i and atom j. Then using the calculated force constant matrices as inputs, we calculated phonon transmission by the NEGF method as described in Ref. [35]. Finally we computed thermal conductance by the Landauer formula[29]

$$\sigma(T) = \frac{\hbar^2}{2\pi k_B T^2} \int_0^{\infty} d\omega \frac{\omega^2 e^{\hbar\omega/(k_B T)}}{(e^{\hbar\omega/(k_B T)} - 1)^2} \Xi(\omega), \quad (1)$$

where $\hbar$ is the reduced Planck constant, k_B is the Boltzmann constant, and T is the temperature. $\Xi(\omega)$ is the transmission for phonon with frequency ω, which can be given from the phonon retarded Green's function $G^r(\omega)$. Further calculation details can be found elsewhere.[35] Thermal conductance per unit area σ/S is used when comparing thermal conduction ability between systems of different sizes. For GNR systems, the cross-sectional area S is defined as $S = W\delta$, where W is the ribbon width and $\delta = 3.35$ Å is the layer separation of graphite.

III. RESULTS AND DISCUSSION

In the following, we will first present results for an experimentally accessible extended defect,[23] which contains a pair of pentagons and one octagon (denoted as "585" hereafter) periodically repeated along the dislocation line (see Fig. 1), then generalize our conclusions by considering other types of extended defects. To see the influence of extended defect orientation, we will study two types of defect systems [depicted in Figs. 1(a) and 1(b)], where the dislocation lines are parallel and perpendicular to the ribbon edges (i.e., the transport direction), respectively. For simplicity, hereafter we label them as "585$^{\parallel}$" and "585$^{\perp}$", respectively.

Thermal transport behavior is found to be insensitive to the detailed location of the extended defect in the GNRs. In "585$^{\parallel}$" of $W \sim 7.3$ nm, as the position of the extended defect varies from the ribbon edge to the middle, the variance in the calculated room-temperature thermal conductance is less than 3% (data not shown). This feature is mainly due to the collective nature of lattice vibration. In "585$^{\perp}$", shifting the position of the extended defect actually does not change the transport system. In the following study we focus on GNRs with an extended defect located in the middle, as shown in Fig. 1.

The room-temperature scaled thermal conductance σ/S of the "585$^{\parallel}$" and "585$^{\perp}$" systems is presented as a function of W in Fig. 1(c). σ/S is found to be insensitive to the variance of W for both systems, indicating an approximately linear width dependence of thermal conductance. This can be explained by the fact that the number of transport channels is roughly proportional to W in most frequency ranges (data not shown). More importantly, there exist considerable differences in the σ/S of "585$^{\parallel}$" and "585$^{\perp}$". At $W \sim 10$ nm, "585$^{\parallel}$" has a room-temperature σ/S of 3.5 nWK^{-1}nm^{-2}, more than 50% higher than that of "585$^{\perp}$", showing that thermal conductance is strongly dependent on the relative direction between the GNR edges and the dislocation line. To further clarify the effects of the defect orientation, we considered two other angles of 30° and 60° between the GNR edge and the dislocation line. It is found that thermal conductance of the 60° system is between values of the parallel and

perpendicular cases (i.e., angles of 0° and 90°), but thermal conductance of the 30° system is even lower than that of "585⊥", showing a complex angle dependence. We did not study more general cases, because a thorough investigation of the angle dependence is computationally difficult and beyond the scope of the present work. Considering the trend that the difference in σ/S shows a weak width dependence, the difference in the thermal conductance σ will grow almost linearly with W, and thus can be very large in wide GNR systems. Our results imply that in graphene with extended defects, large thermal conductance/resistance can be obtained once the transport direction is parallel/perpendicular to the dislocation line. Consequently, thermal conductance can be tuned over wide ranges simply by controlling the transport direction.

Embedding extended defects into GNRs reduces thermal conductance substantially. To quantify the defect-induced thermal conductance reduction, we choose pristine zigzag GNRs (ZGNRs) and armchair GNRs (AGNRs) as reference systems for "585∥" and "585⊥", respectively. Note that ZGNRs/AGNRs have the same zigzag/armchair edges as "585∥"/"585⊥". The room-temperature σ/S of pristine GNRs, as reported in Ref. 36, shows observable size effects when $W < 2$ nm, weak width dependence when $W > 2$ nm, and an intrinsic anisotropy of thermal conductance with the room temperature σ/S of ZGNRs up to 30% larger than that of AGNRs. Introducing extended defects into GNRs significantly decreases their thermal conductance. For instance, the room-temperature σ/S of the ZGNR/AGNR decreases by 16%/37%

to the value of 3.5/2.3 nWK^{-1} nm^{-2} in "585∥"/"585⊥" at $W \sim 10$ nm. What is the underlying mechanism of the defect-induced thermal conductance reduction? To answer this question, we analyze the phonon transmission function.

The phonon transmission functions of the GNR systems ($W = 7.3$ nm) with and without the extended defect are compared in Figs. 2(a) and 2(b). In "585∥", the defect-induced phonon transmission reduction is observable at regions of 150–1000 cm^{-1} and 1300–1700 cm^{-1}. In contrast, the reduction is more significant in "585⊥", where the extended defect affects phonons in wider frequency ranges ($\omega > 150$ cm^{-1}) and causes a larger decrease in the phonon transmission. As shown in Fig. 2(c), the ratio between phonon transmissions of AGNR with "585⊥" defect and pristine AGNR ($\Xi_{585\perp}/\Xi_{AGNR}$) is lower than 1 in all the frequency range, due to the structural defect-induced phonon scattering. The reduction of phonon transmission is small in the low-frequency region but large in the high-frequency region, consistent with Serov *et al.*'s results.[26] Our results indicate that low-frequency phonons transport (quasi-)ballistically in the presence of defect scattering, whereas most high-frequency phonons are strongly scattered by local defects and their transport approaches the diffusive limit as the strength of defect scattering gets stronger (e.g., by increasing the number of defects) and the phonon mean free path becomes shorter than the transport length. These features of phonon transmission are reflected in the behavior of thermal conductance, which is actually a weighted integration of the phonon transmission function [see Eq. (1)].
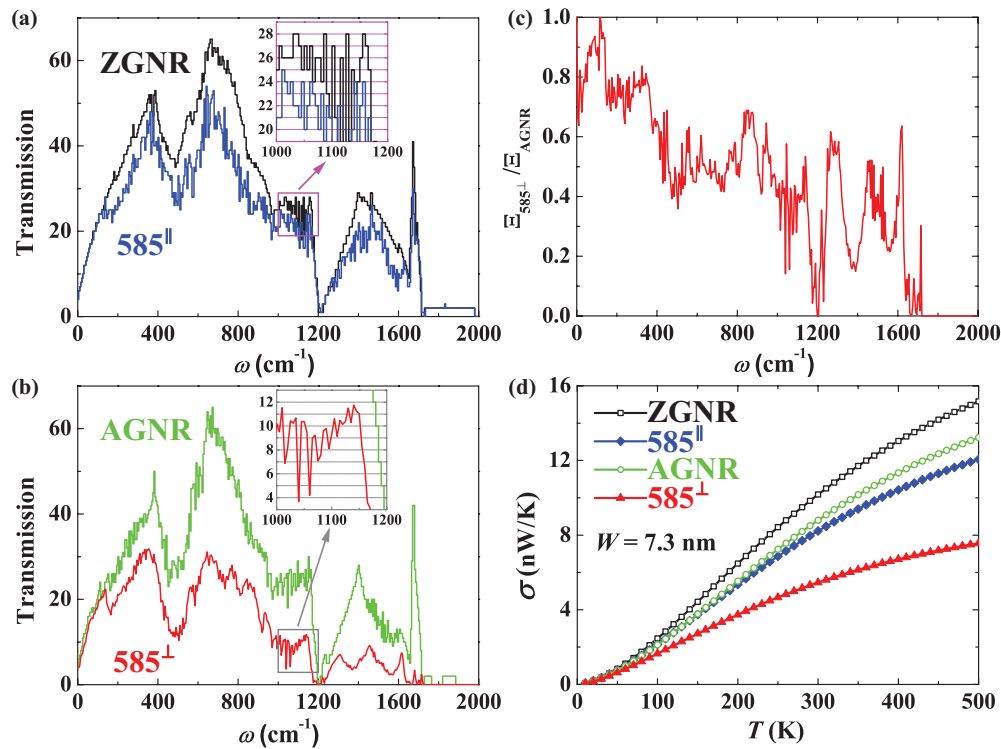

FIG. 2. (Color online) (a), (b) Phonon transmission versus phonon frequency ω for graphene nanoribbons (GNRs) of width $W = 7.3$ nm. (c) Phonon transmission in an armchair GNR (AGNR) with an extended line defect normalized by transmission of the same AGNR without defects ($\Xi_{585\perp}/\Xi_{AGNR}$) as a function of phonon frequency. (d) Thermal conductance σ versus temperature T for GNRs of width $W = 7.3$ nm. The phonon transmission functions are compared (a) between pristine zigzag GNR (ZGNR) and "585∥", and (b) between pristine AGNR and "585⊥". The insets of (a) and (b) show the integer and noninteger phonon transmission in the specific frequency range for "585∥" and "585⊥", respectively.

As shown in Fig. 2(d), the differences in thermal conductance between GNRs with and without the extended defect are nearly zero at low temperatures (i.e., $T < 50$ K) and gradually grow with increasing temperature.

Then we show that the extended defect induced phonon transmission reduction in "585$^{\parallel}$" and "585$^{\perp}$" is caused by fundamentally different mechanisms. Introducing defects usually breaks the periodicity of the transport system and thus induces phonon scattering that suppresses phonon transmission. This is the case in "585$^{\perp}$", which has noninteger phonon transmission [see the inset of Fig. 2(b)] caused by defect-induced phonon scattering. While in "585$^{\parallel}$", the periodicity of the structure is preserved with a periodic array of defects, and no phonon scattering is induced by the structural imperfection, as evidenced by its integer phonon transmission [see the inset of Fig. 2(a)]. Embedding the extended defect into GNRs, however, changes the degree of phonon localization. This is not straightforward. To elucidate the issue, let us first look at pristine GNRs. There the ribbon edges that have a bonding configuration different from its bulk reference (i.e., graphene) can be viewed as extended defects. Previous works find that the bonding configuration at edges affects the degree of phonon localization.[36,37] Specifically, phonons in AGNRs behave more localized than in ZGNRs.[36] Generally, phonons of GNRs would be more localized if the change in the bond strength, caused by the formation of edges, is larger along the transport direction (i.e., the ribbon edge). When cutting graphene into GNRs, the edge bonds that are broken have a significant component along the ribbon edge in AGNRs, while those broken bonds are perpendicular to the ribbon edge in ZGNRs. This rationalizes stronger phonon localization in AGNRs than in ZGNRs. Similarly, the large difference in the bonding configuration between the extended "585" defect and graphene could explain the more localized phonons and thus lower phonon transmission in "585$^{\parallel}$" than in the reference ZGNR.

Since the essential difference between "585$^{\parallel}$" and ZGNR lies in the degree of phonon localization caused by embedding extended defect, one may expect that their thermal conductance per unit area (σ/S) will converge when the width is large enough. Previous work showed an intrinsic anisotropy of thermal conductance in AGNR and ZGNR due to different boundary conditions.[36] Such an anisotropy disappears in pristine GNRs with very large width ($\sim$140 nm at 300 K), and the thermal conductance will converge to the isotropic value of the graphene sheet. This is closely related to the long-range nature of phonons which allows for long-range edge/boundary effects on phonon transport. In analogy, the parallel line defect should have a long-range influence on the thermal conductance, similar to the boundary effects in pristine GNRs. This is evidenced by a gradual change in the calculated σ/S as presented in Fig. 1. Note that a direct calculation of σ/S to determine the critical width at which the difference between ZGNR and "585$^{\parallel}$" disappears is beyond our computational capabilities. Instead, we made a rough estimation by using linear regression to fit the data from 5 to 15 nm for "585$^{\parallel}$" and ZGNR, and found that the critical width is about 53 nm.

Importantly, thermal conductance of the "585$^{\perp}$" system exhibits an interesting dependence on the length of the line defect. In order to show the defect-length effects, we calculated the thermal conductance for "585$^{\perp}$" systems with a fixed
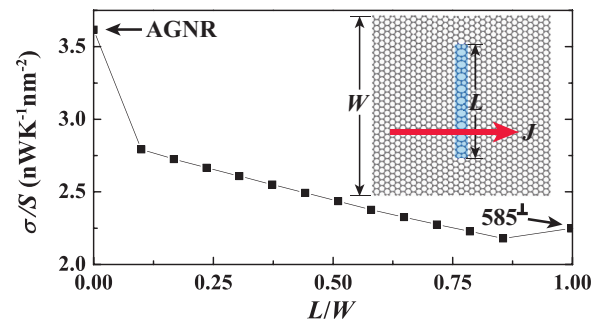

FIG. 3. (Color online) Thermal conductance per unit area (σ/S) at 300 K versus the L/W ratio of "585" defects lying perpendicular to the ribbon edge. The inset shows the thermal transport system of width W with a line defect of length L.

width but different lengths of the line defect (not extending across the entire system, see the inset of Fig. 3). The results are summarized in Fig. 3. By varying the length of "585$^{\perp}$" in the GNR, the thermal conductance can be tuned nearly monotonously from the high value of pure AGNR to the low limit of "585$^{\perp}$". It can be also seen that an obvious jump appears around $L/W = 0$, implying that introducing local defect to break the perfection of the pristine GNR can cause a significant decrease of thermal conductance. Moreover, increasing the length of defects can further decrease thermal conductance linearly, indicating that an extended defect can induce stronger phonon scattering. Our analysis strongly suggests that extended defects would be more effective in tuning thermal conductance over wide ranges.

In addition to the extended "585" defect, we also investigated other types of extended defects composed of the "A57Z",[38] "d5d7"[39] and "t5t7"[39] defects, respectively (with the same notation as in the references; see Fig. 4 for

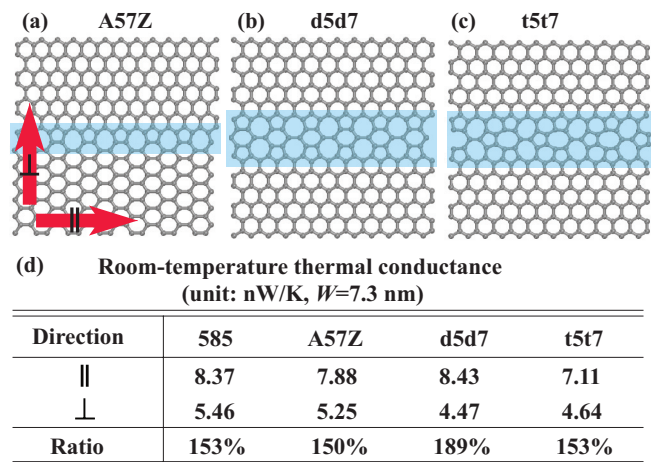| Direction	585	A57Z	d5d7	t5t7
$\parallel$	8.37	7.88	8.43	7.11
$\perp$	5.46	5.25	4.47	4.64
Ratio	153%	150%	189%	153%

FIG. 4. (Color online) (a)–(c) Schematic of graphene nanoribbons (GNRs) with different extended defects. (a) The "A57Z" extend defect is a linear array of pentagons and heptagons that join an armchair GNR to a zigzag GNR (Ref. 38). (b)/(c) The "d5d7"/"t5t7" extend defect contains a series of double/triple pentagons and double/triple heptagons (Ref. 39). (d) Room-temperature thermal conductance of GNRs ($W = 7.3$ nm) with different extended defects parallel ("$\parallel$") and perpendicular ("$\perp$") to the ribbon edges, and the ratio of their thermal conductance ("$\parallel$" to "$\perp$").

atomic structures). Similar as in Fig. 1(c), σ/S of GNRs with the extended defect parallel and perpendicular to the transport direction is compared as a function of W (data not shown). Since σ/S of both orientations is weakly dependent on W when W is larger than 2 nm, we only present the calculated room-temperature thermal conductance in Fig. 4(d) for defective GNRs with $W = 7.3$ nm. The parallel case gives room-temperature thermal conductance more than 50% higher than the perpendicular case for all the considered extended defects. The difference could be even as large as 89% in GNRs with the extended "d5d7" defect. These results show that the thermal conductance depends strongly on the orientation of the extended defect, regardless of the detailed structure of the embedded extended defect. Although wide-range-tunable thermal conductances have been demonstrated for a single extended line defect, further enhancement in the changing range is possible. This could be realized, for instance, by introducing more extended defects into the system. Then the extra degree of freedom of combining different types of defects, that could scatter phonons in a synergistic way, would open different possibilities to tune thermal conductance.

IV. CONCLUSION

In summary, we have theoretically demonstrated that thermal conductance can be tuned over wide ranges by controlling the direction and bonding configuration of the embedded extended defect in GNRs, whereas it is insensitive to the location of the defect within the ribbon. Moreover, we reveal that the thermal-conduction tuning is achieved through two fundamentally different mechanisms (i.e., modifying phonon spectra and adjusting the strength of phonon scattering). The proposed approach of tuning thermal conduction via extended defects, found to be efficient in GNRs, is expected to be applicable to other materials.

*Present address: Fritz-Haber-Institut der Max-Planck-Gesellschaft, Faradayweg 4-6, D-14195 Berlin-Dahlem, Germany; yongxu@fhi-berlin.mpg.de

†dwh@phys.tsinghua.edu.cn

[1]E. Pop, S. Sinha, and K. E. Goodson, Proc. IEEE **94**, 1587 (2006).

[2]N. P. Padture, M. Gell, and E. H. Jordan, Science **296**, 280 (2002).

[3]G. J. Snyder and E. S. Toberer, Nat. Mater. **7**, 105 (2008).

[4]T. Yao, Appl. Phys. Lett. **51**, 1798 (1987).

[5]W. Kim, R. Wang, and A. Majumdar, Nano Today **2**, 40 (2007).

[6]G. Zhang and B. Li, J. Chem. Phys. **123**, 114714 (2005).

[7]C. W. Chang, A. M. Fennimore, A. Afanasiev, D. Okawa, T. Ikuno, H. Garcia, D. Li, A. Majumdar, and A. Zettl, Phys. Rev. Lett. **97**, 085901 (2006).

[8]I. Savić, N. Mingo, and D. A. Stewart, Phys. Rev. Lett. **101**, 165502 (2008).

[9]N. Yang, G. Zhang, and B. Li, Nano Lett. **8**, 276 (2008).

[10]N. Mingo, D. A. Stewart, D. A. Broido, and D. Srivastava, Phys. Rev. B **77**, 033418 (2008).

[11]M. Morooka, T. Yamamoto, and K. Watanabe, Phys. Rev. B **77**, 033412 (2008).

[12]J. Wang, L. Li, and J.-S. Wang, Appl. Phys. Lett. **99**, 091905 (2011).

[13]W. Kim, J. Zide, A. Gossard, D. Klenov, S. Stemmer, A. Shakouri, and A. Majumdar, Phys. Rev. Lett. **96**, 045901 (2006).

[14]D. Li, Y. Wu, P. Kim, L. Shi, P. Yang, and A. Majumdar, Appl. Phys. Lett. **83**, 2934 (2003).

[15]A. H. Castro Neto, F. Guinea, N. M. R. Peres, K. S. Novoselov, and A. K. Geim, Rev. Mod. Phys. **81**, 109 (2009).

[16]A. A. Balandin, Nat. Mater. **10**, 569 (2011).

[17]E. Pop, V. Varsheny, and A. K. Roy, MRS Bulletin **37**, 1273 (2012).

[18]Q. Yan, B. Huang, J. Yu, F. Zheng, J. Zang, J. Wu, B.-L. Gu, F. Liu, and W. Duan, Nano Lett. **7**, 1469 (2007).

[19]X. Li, X. Wang, L. Zhang, S. Lee, and H. Dai, Science **319**, 1229 (2008).

[20]D. V. Kosynkin, A. L. Higginbotham, A. Sinitskii, J. R. Lomeda, A. Dimiev, B. K. Price, and J. M. Tour, Nature (London) **458**, 872 (2009).

[21]J. Coraux, A. T. N'Diaye, M. Engler, C. Busse, D. Wall, N. Buckanie, F.-J. Meyer zu Heringdorf, R. van Gastel, B. Poelsema, and T. Michely, New J. Phys. **11**, 023006 (2009).

[22]H. J. Park, J. Meyer, S. Roth, and V. Skákalová, Carbon **48**, 1088 (2010).

[23]J. Lahiri, Y. Lin, P. Bozkurt, I. I. Oleynik, and M. Batzill, Nat. Nanotech. **5**, 326 (2010).

[24]A. Bagri, S.-P. Kim, R. S. Ruoff, and V. B. Shenoy, Nano Lett. **11**, 3917 (2011).

[25]Y. Lu and J. Guo, Appl. Phys. Lett. **101**, 043112 (2012).

[26]A. Y. Serov, Z.-Y. Ong, and E. Pop, Appl. Phys. Lett. **102**, 033104 (2013).

[27]T. Yamamoto and K. Watanabe, Phys. Rev. Lett. **96**, 255503 (2006).

[28]N. Mingo, Phys. Rev. B **74**, 125402 (2006).

[29]J.-S. Wang, J. Wang, and J. T. Lü, Eur. Phys. J. B **62**, 381 (2008).

[30]Y. Xu, J.-S. Wang, W. Duan, B.-L. Gu, and B. Li, Phys. Rev. B **78**, 224303 (2008).

[31]D. W. Brenner, O. A. Shenderova, J. A. Harrison, S. J. Stuart, B. Ni, and S. B. Sinnott, J. Phys.: Condens. Matter **14**, 783 (2002).

[32]J. D. Gale, J. Chem. Soc., Faraday Trans. **93**, 629 (1997).

[33]M. Vandescuren, P. Hermet, V. Meunier, L. Henrard, and Ph. Lambin, Phys. Rev. B **78**, 195401 (2008).

[34]S. Ghosh, I. Calizo, D. Teweldebrhan, E. P. Pokatilov, D. L. Nika, A. A. Balandin, W. Bao, F. Miao, and C. N. Lau, Appl. Phys. Lett. **92**, 151911 (2008).

[35] Y. Xu, X. Chen, J.-S. Wang, B.-L. Gu, and W. Duan, Phys. Rev. B **81**, 195425 (2010).

[36] Y. Xu, X. Chen, B.-L. Gu, and W. Duan, Appl. Phys. Lett. **95**, 233116 (2009).

[37] Z. W. Tan, J.-S. Wang, and C. K. Gan, Nano Lett. **11**, 214 (2011).

[38] A. R. Botello-Méndez, E. Cruz-Silva, F. López-Urías, B. G. Sumpter, V. Meunier, M. Terrones, and H. Terrones, ACS Nano **3**, 3606 (2009).

[39] A. R. Botello-Méndez, X. Declerck, M. Terrones, H. Terrones, and J.-C. Charlier, Nanoscale **3**, 2868 (2011).